An Investigation on the Fatigue Performance of Hydraulic Gate Wheels

Dimos Polyzois and Abdul Nabi Lashari
Department of Civil Engineering, University of Manitoba
75B-Chancellor Circle, Winnipeg, MB, R3T 5V6, Canada
polyzoi@cc.umanitoba.ca

ABSTRACT

Manitoba Hydro is Canada's largest hydro utility company currently owning fourteen hydropower-generating stations with a total capacity of over 7500 MW. Both emergency intake gates and spillway gates are used in each. These are fixed-wheel gates with wheels mounted on both sides that roll on roller paths plates. Environmental corrosion along with high wheel loads cause differences in the profile of the roller path surface. Combined with the relatively high torsional stiffness of the gate end girders, a condition of wheel load redistribution occurs where some wheels are relieved of load while others are loaded beyond their maximum design values. These loads can be as high as two to three times larger than the original design loading. Failure of one wheel could jeopardize the overall operation of the gate. Furthermore, the frequent opening and closing of these gates result in changes in the stress profile in both wheels and roller path plates that, potentially, could lead to failure. Currently, design guidelines for gate wheels and roller paths do not consider the fatigue life of these elements.

An experimental investigation was carried out at the University of Manitoba in Winnipeg, Canada, which involved the testing of three wheels and six roller path plates under cyclic loading. The wheels were 838 mm in diameter while the roller path plates were 381 x 178 x 51 mm. One of the wheels was made of cast iron while the other two were made of forged steel. The material in two of the roller path plates was ASTM C 1040 with no heat treatment. The material in the other plates was ASTM C 1045 with heat treatment. The wheels were subjected to a radial load of, approximately, 825 kN that remained fairly constant while the wheels were "rolled" over the roller path for up to one million cycles. The tensile strain on the cast iron wheel ranged from 103 $\mu\varepsilon$ to 2057 $\mu\varepsilon$ while the tensile strain on the forged steel ranged from 4 $\mu\varepsilon$ to 206 $\mu\varepsilon$. Tensile strains were observed in almost all the strain gauges installed on the roller path plates. Those roller path plates which were not heat treated exhibited a maximum indentation of 1.48 mm and 1.21 mm, respectively, after one million cycles, while the roller path plates that were heat treated suffered a much smaller surface indentation which ranged from 0.02 mm to 0.11 mm after 400,000 cycles. The test results demonstrated that cast iron wheels performed very poorly under fatigue loading while heat-treated forged steel wheels performed well.

Introduction

Fixed-wheel gates have been extensively used in many water resource development projects all over the world. The term fixed-wheel gate applies to a rectangular gate with wheels mounted on the gate, as contrasted with an earlier type using roller chains independent of the gate leaf. The hydrostatic load is transferred through a skin plate, onto a structural system of diaphragms, horizontal girders,

and vertical end girders that are supported on wheels [1]. The water thrust on the gate is transferred by the wheels to the roller path plates in the gate slots, fastened to track bases embedded in concrete of the structure, and the wheels rotate on the track as the gate is operated. Consequently, the wheel is a critical component of the gate assembly. Environmental corrosion and high wheel loads cause differences in the profile of the roller path surface. Combined with the relatively high torsional stiffness of the gate end girders, a condition of wheel load redistribution occurs where some wheels are relieved of load and other wheels are loaded beyond the maximum values for which they have been designed. These loads can be as high as two to three times larger as the original design loading. Failure of one wheel could jeopardize the overall operation of the gate [1]. While the design of various gate structural components is carried out on the basis of established national standards, the design of gate wheels involves the use of an empirical formula, based on Brinell hardness, to obtain the initial wheel diameter and the tread width [2]. Tread surface Hertzian contact stresses and subsurface shear stresses are computed using methods developed by Thomas and Hoersch [3]. Although the Noonan and Strange formula was based on tests involving small-diameter cylindrical forged steel wheels, it has been subsequently adopted for the design of large-diameter crowned wrought-steel wheels, some in excess of 760 mm in diameter. The applicability of this formula to crowned wheels is questionable. Furthermore, this formula provides no information on the fatigue life of wheels or the relationship between the safe working loads and ultimate load capacity of the wheels, thereby making the safe wheel capacity unknown [1].

Fatigue Behavior of Solids in Contact

When two solid bodies press against each other over a limited area of contact, high stresses are developed. These contact stresses, on or somewhat beneath the surface of contact, could result in failure of one or both of the bodies. For example, contact stresses may be significant in the area between a locomotive wheel and the railroad rail; between a roller or ball and its race in a bearing; between the teeth of a pair of gears in mesh; between the cam and valve tappets of a gasoline engine; [4]. In many situations, as in the case of these examples, the members do not necessarily remain in fixed contact. In fact, the contact stresses are often cyclic in nature and are repeated a very large number of times, often resulting in a fatigue failure that starts as a localized fracture (crack) associated with localized stresses. The fact that contact stresses frequently lead to fatigue failure largely explains why these stresses may limit the load-carrying capacity of the members in contact and hence may be the significant stresses in the bodies. For example, a railroad rail sometimes fails as a result of contact stresses. The failure starts as a localized fracture in the form of a minute transverse crack at a point in the head of the rail, somewhat beneath the surface of contact between the rail and locomotive wheel, and progresses outwardly under the influence of the repeated wheel loads until the entire rail cracks or fractures. This fracture is called a *transverse fissure failure* [4]. Contact stresses can also cause pitting at the surface of contact. The bottom of such pits is often located at the depth of maximum shearing stress. This is probably the cause of failure of a number of cast iron wheels used by Manitoba Hydro.

The principal stresses at the contact area are higher than the stresses at a point beneath the contact area; whereas the maximum shearing stress is greater at a point a small depth from the contact surface. Due to fabrication errors or due to deflection of the gate girders, however, it is possible that the direction of the roll is not coincident with direction of the roller path. In this case, frictional forces develop between the wheel and the roller path. The addition of these forces causes a change in the shearing stresses in the contact area. Furthermore, the location of the point at which the maximum shearing stresses occur moves from beneath the surface of the contact towards the contact area. Fig. 1 shows the distribution of the principal stresses at the contact surface of a wheel with a coefficient of friction of ⅓. The figure also shows that the frictional force cause an increase in the principal stresses by 40%. It is important to note that the principal stresses σ_1 and σ_2 are tensile

stresses near the edge of the contact area. These values are sometimes quite large. The presence of the tensile stresses result in fatigue failure by pitting of bearing surfaces under repeated loads [4].
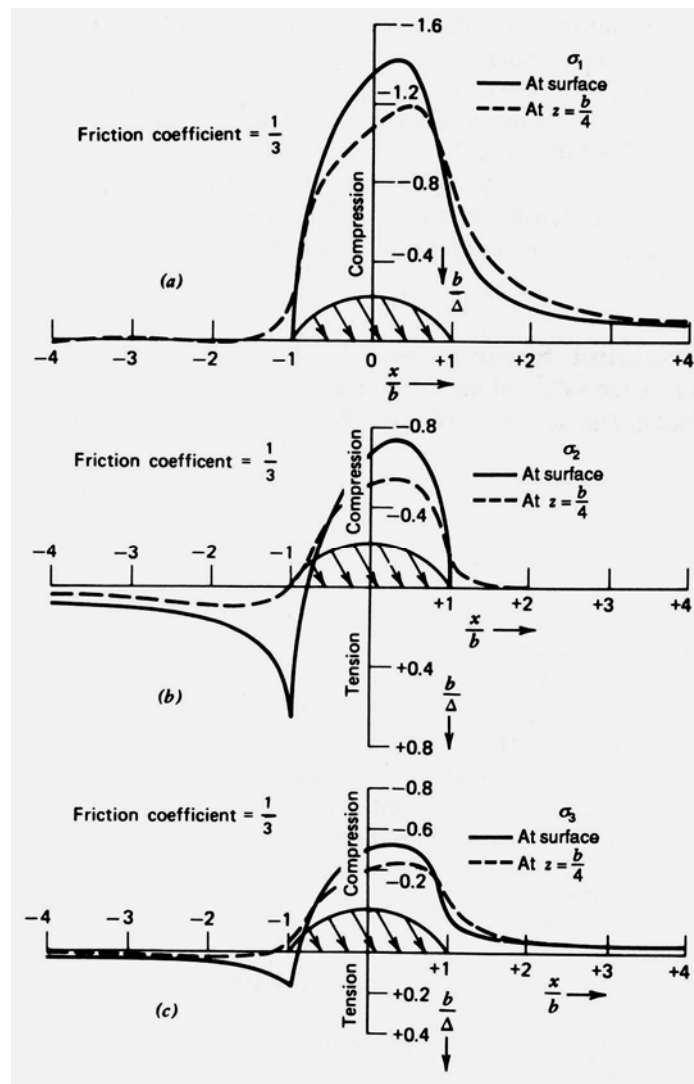

Fig. 1. Distribution of contact stresses [4]

Experimental Program

The experimental program at the University of Manitoba, Canada, involved the testing of three wheels and six roller path plates under cyclic loading. The wheels were 838 mm in diameter along with an 89 mm flange (rim) thickness (depth) and a crown radius of 914 mm. One of the wheels (Wheel R1) was made of cast iron and the other two (Wheels R2 & R3) were made of forged steel. Six rectangular steel plates (P1 through P6), measuring 381 x 178 mm with a thickness of 51 mm were used as roller path plates in this research program. The material in two of the roller path plates (P1 & P2) was ASTM C 1040 with no heat treatment, whereas, the material in the other four plates (P3 through P6) was ASTM C 1045 with heat treatment. The heat- treated plates had reported yield strength of 238 MPa and a tensile strength of 510 MPa.

A unique test set up, shown in Fig. 2, was specially designed and constructed for this experimental program. The hydraulic pressure generated by the pump was transferred to a hydraulic actuator through two hydraulic hoses, one for forward motion of the actuator piston rod and other for backward motion of the actuator piston rod. The 15 kW (20 horse-power) motor of the pump was

designed to generate a maximum pressure of 17.2 MPa. This pressure value corresponded to a lateral load of 184.5 kN on the hydraulic actuator. The purpose of the hydraulic actuator was to deliver a lateral cyclic load through a 51 mm diameter solid steel piston rod, which was attached to 127 x 102 x 76 mm solid steel plate through threads, shown in Fig. 3. This solid plate was attached to an 863 x 609 x 76 mm solid steel plate through welding and four countersunk steel bolts in order to avoid any kind of failure during cyclic loading. In order for the actuator to deliver the cyclic loading continuously and without interruption, two small magnetic sensors were used. These magnetic sensors were installed on a small steel frame mounted on the hydraulic actuator and wired to the power panel switchboard of the pump. The hydraulic actuator was attached to a steel frame through four 19 mm diameter steel bolts.

Fig. 2. Test set-up	Fig. 3 Wheel Under Testing

In order to support the roller path plates two 863 x 609 x 76 mm steel plates were used in this unique test set-up, as shown in Fig. 3. One plate was permanently attached to the 609 mm thick strong concrete wall of the Structural Engineering Laboratory. The other plate was attached to the 51 mm diameter solid steel piston rod of the hydraulic actuator. The roller path plates were attached to this plate through steel bolts. A series of high strength solid round bars was placed between the two plates to allow the plate with the roller path to roll freely back and forth. The roller was placed in this steel fixture horizontally and secured in place with a long solid steel shaft, 152 mm in diameter and 495 mm in length, inserted through the steel fixture and the 152 mm diameter hole of the wheel. A radial compressive load equivalent to service load was applied on the wheels by compressing the whole steel fixture against the roller path plate through four high strength rods which ran through the 609 mm thick strong concrete wall. These four high strength rods were calibrated in order to monitor the axial load during testing. Four hydraulic jacks were used to apply the axial load. The average radial load on Wheel R1, side A during cyclic testing was 825 KN.

Strain gauges were installed on all wheels and roller path plates in order to monitor and record the strain values during cyclic loading. Each wheel was tested with two different roller path plates utilizing two opposite sides of the wheel. The strain gauge location for Wheel R1 – Side A are shown in Fig. 4. All strain gauges were connected to a computer controlled data acquisition system.

The wheels were tested at two opposite locations labeled as side "A" and side "B". For each cyclic test, a wheel was in contact with the roller path on one side only. Wheel R1 was tested to a million cycles on side "A" (Test T1A) and 818,726 cycles on side "B" (Test T1B) with roller path Plates P1 and P2, respectively. The test was continuous and uninterrupted during this trend. Wheel R2 was tested continuously to 220,000 cycles on side "A" (Test T2A) and 200,000 cycles on side "B" (Test

T2B) with roller path Plates P3 and P4, respectively. After completing each test, the test set-up was dismantled and indentation profiles in the roller path plates were recorded. Wheel R3 was tested for 200,000 cycles on side "A" with roller path plate P5 (Test T3A1). After completing 200,000 cycles, the test setup was dismantled and indentation profiles in the roller path plate P5 were measured. After this test, Wheel R3 was re-loaded on the same location side "A" along with same roller path plate P5 and was re-tested for an additional 200,000 cycles (Test T3A2). A similar procedure was used to test side "B" of the same Wheel R3 with roller path plate P6 up to 200,000 cycles (T3B1) and up to an additional 200,000 cycles (T3B2).
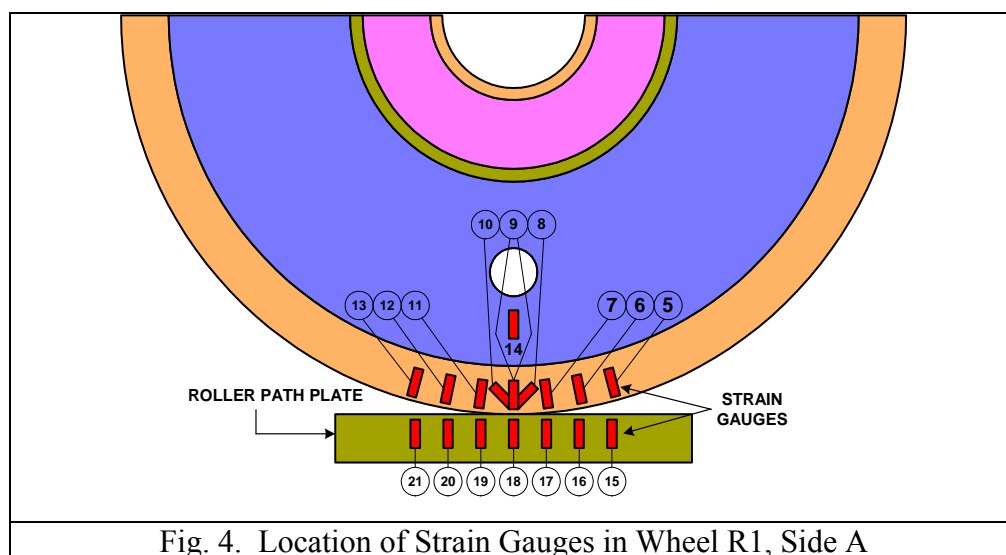

Fig. 4. Location of Strain Gauges in Wheel R1, Side A

Wheel R1 was rolled back and forth on roller path Plates P1 and P2 for a total circumferential distance of 75 mm or 37.5 mm from either side of the initial point of contact. Wheels R2 and R3 were rolled back and forth on roller path plates for a total circumferential distance of 50 mm or 25 mm from either side of the initial point of contact. At the end of each cyclic test, the test-setup was dismantled and indentation measurements were taken for each roller path plate using a dial gauge.

Results

Prior to testing, the hardness of the rollers and the roller path plates were measured. The hardness measurements indicated that the wheel hardness profile for Wheel R1 (cast iron) varied from 391 BHN at the rolling surface to 219 BHN at 38 mm away from the rolling surface. The hardness for Wheel R2 (wrought steel) varied from 373 BHN at the rolling surface to 326 BHN at 63 mm away from the rolling surface. The hardness for Wheel R3 (wrought steel) varied from 473 BHN at the rolling surface to 428 BHN at 38 mm away from the rolling surface.

Maximum tensile strains were observed in the strain gauges installed on the rim surface of the wheel when these strain gauges were farthest away from the contact point and minimum tensile strains were recorded when the strain gauges were either in contact with the roller path plate or very close to the contact point. The reason for minimum tensile strains, when the strain gauges were either in contact or very close to the contact point, was that the rolling rim surface had a depth of 89 mm (3½ in.) and a crown radius of 914 mm (36 in.) along with a chamfer of 6.4 mm (¼ in.) long, inclined at 45º in between the rolling surface and rim surface, as shown in Fig. 5.
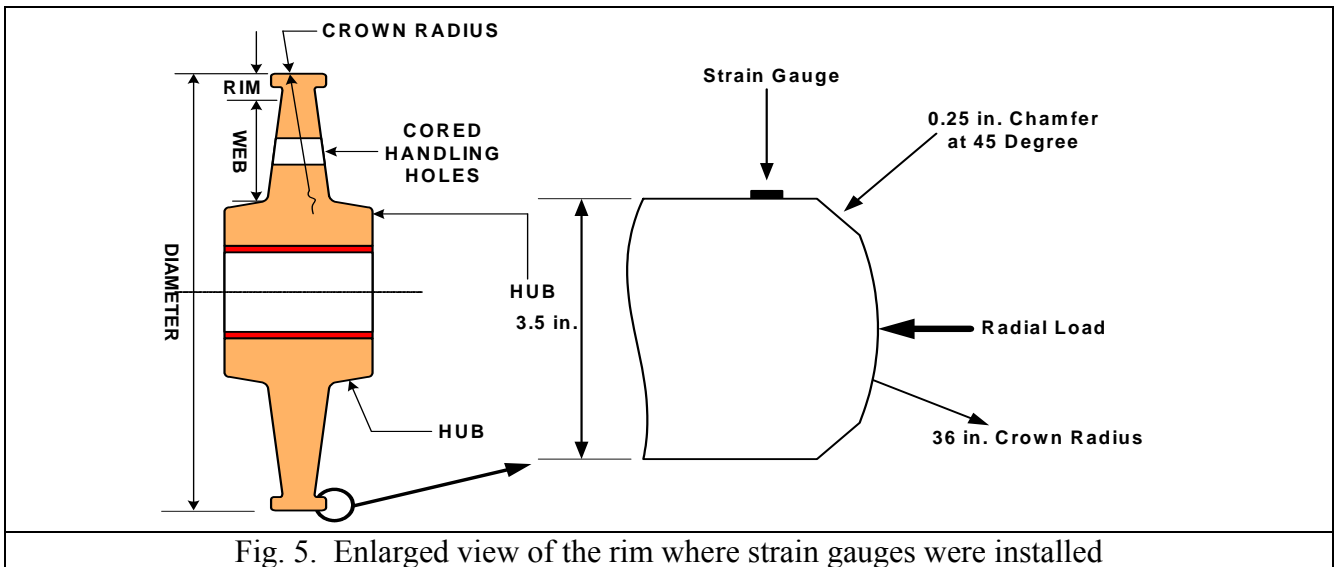
Fig. 5. Enlarged view of the rim where strain gauges were installed

As shown in Fig. 6, the strain recorded by strain gauge 9 in Test T1A, varied from 842 $\mu\varepsilon$ (in tension), when the strain gauge was in direct alignment with the point in contact with the roller path, to 1340 $\mu\varepsilon$ (in tension), when the strain gauge was the farthest away from the contact point. The location of strain gauge 9 during the first cycle is illustrated in Fig. 7. In the majority of the strain gauges installed on the rim surface of the wheel, it was found that with the increase in the number of cycles, the strain dropped from a high tensile strain to a low tensile strain or even to compressive strain. An example is shown in Fig. 8, where a continuous drop in the micro-strain was observed in strain gauge 6 up to 500,000 cycles. After that strain level, the strain remained constant until the test was stopped at one million cycles. There are two interesting observations that are of importance to note. First, the strain difference between the minimum and the maximum values became smaller as the number of cycles of loading increased reaching a constant value after a certain number of cycles. Second, both the maximum and the minimum strain values decreased as the number of cycles increased, reaching a constant value after a certain number of cycles, for all strain gauges installed on the rim surface except strain gauges 8 and 10, which were part of rosette strain gauge and were placed at 45° to a plane perpendicular to the rolling surface of roller path plate.
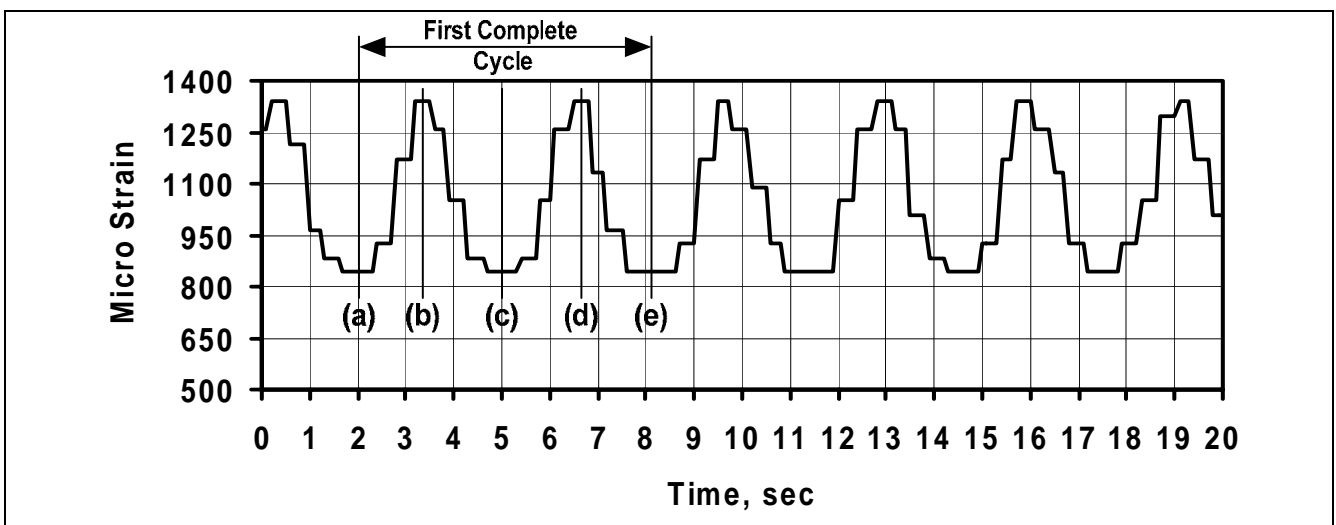

Fig.6. Strain recorded by gauge 9 in Wheel R1, side A, during the first three cycles
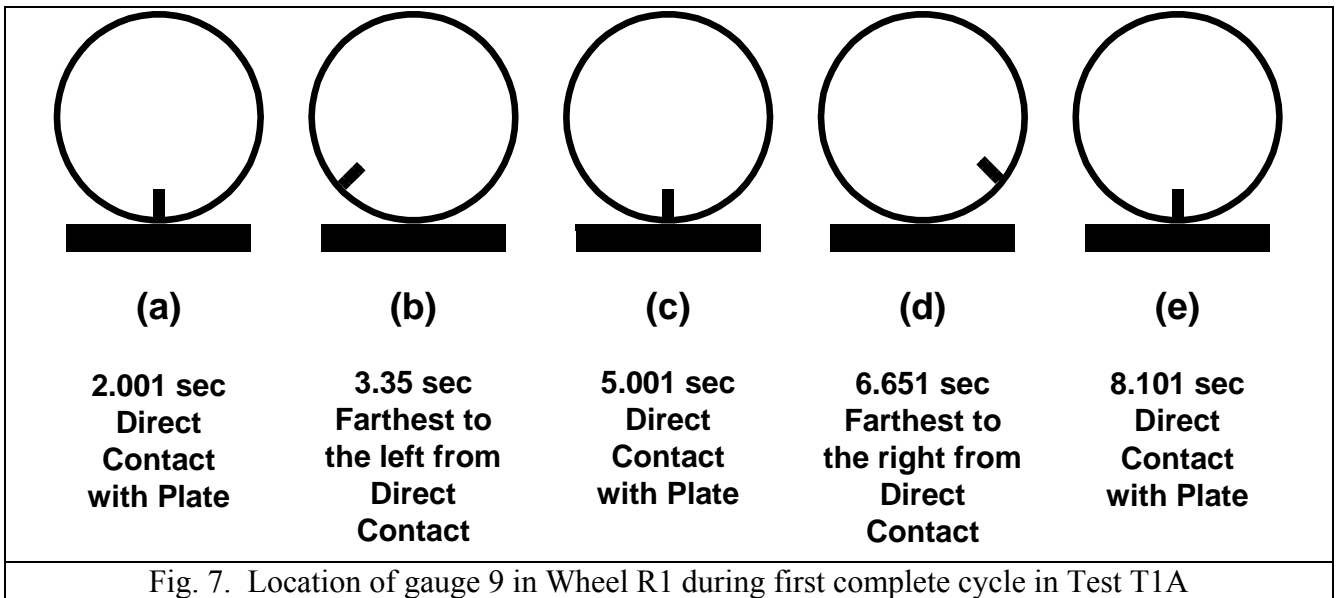
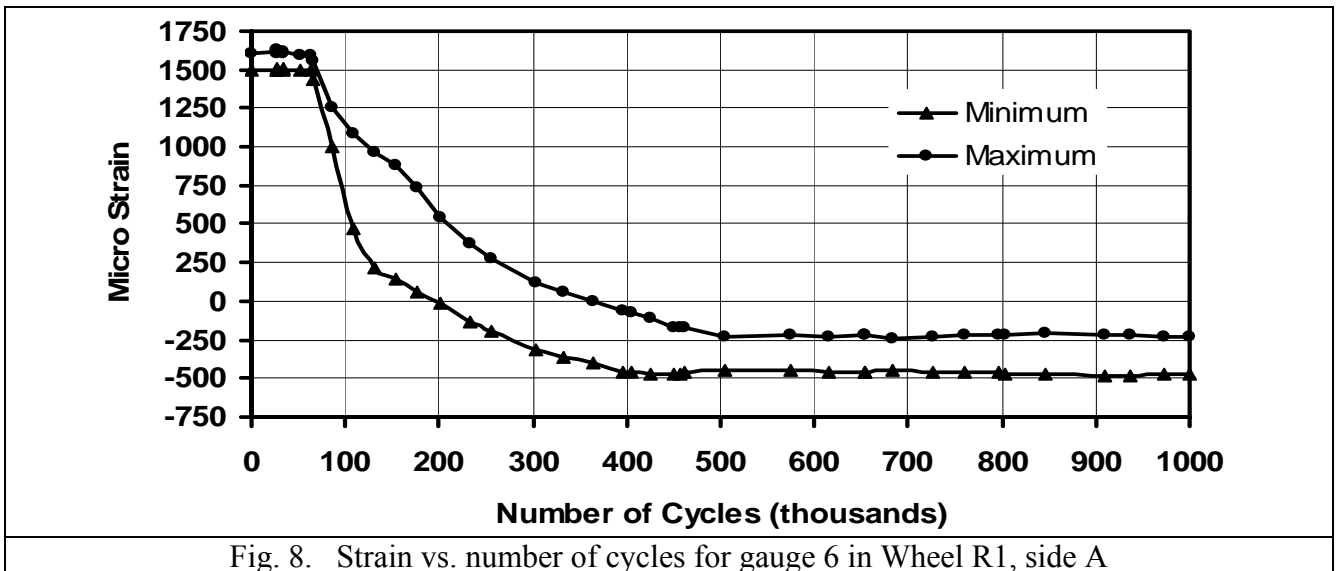Fig. 7. Location of gauge 9 in Wheel R1 during first complete cycle in Test T1A

Fig. 8. Strain vs. number of cycles for gauge 6 in Wheel R1, side A

Since strain gauge 14 was installed in the web area of Wheel R1, side A, and 91.4 mm away from the contact area of the rim rolling surface, it showed no significant change in the strain values during cyclic testing. The strain differences between the maximum and the minimum at each strain gauge location for Wheel R1, after the first and last cycle of loading, are listed in Table 1. With the exception of strain gauge 14, tensile strain ranged from 103 με to 1664 με, whereas the compressive strain ranged from 43 με to 471 με for the Test T1A.

The test results for Wheels R2 and R3 were very much similar to that of Wheel R1. However, the strain values recorded in Wheel R2 and R3 were much lower than those of Wheel R1. The tensile strain ranged from 7 με to 350 με, whereas, the compressive strain ranged from 15 με to 474 με in R2. The tensile strain ranged from 4 με to 176 με, whereas, the compressive strain ranged from 1 με to 157 με in Wheel R3. Tensile strains were observed in almost all the strain gauges installed on the roller path plates.

Table 1. Micro-Strains on Side A of Wheel R1 (Cast Iron), Test 1A

Strain Gauge	At 1st Cycle			At 1,000,000 Cycle		
	Min.	Max.	Differ.	Min.	Max.	Differ.
5	1414	1520	106	384	514	130
6	1498	1605	107	-471	-228	244
7	236	824	588	-43	103	146
8	153	1293	1140	1004	1573	569
9	842	1340	498	562	716	154
10	383	1554	1171	754	1220	466
11	616	833	217	-343	-196	147
12	1544	1751	207	1513	1693	180
13	1542	1664	122	1497	1609	112
14	-1658	-1363	295	-1813	-1465	348

As discussed earlier, indentation measurements were taken on the roller path plates. Path plate P1 exhibited a maximum indentation depth of 1.48 mm after one million cycles, whereas, the indentation in roller path Plate P2 was 1.21 mm after, approximately, 800,000 cycles. In roller path Plates P3 through P6, which were heat-treated, the indentation ranged from 0.02 mm after 200,000 cycles to 0.12 mm after 400,000 cycles.

The contact area on side A of Wheel R1, which was subjected to one million cycles of repeated loading, is shown in Fig. 9. Two sets of major and minor cracks are evident in this figure. Almost similar trend and behavior was observed in the crack pattern of Wheel R1, side B, which was subjected to 818,726 cycles of repeated loading. The tested contact area of Wheel R2 after 200,000 cycles is shown in Fig. 10. There was no sign of any kind of crack or deformation in the tested contact areas of either Wheel R2 or R3. Cracks were also evident in the roller path Plates P1 and P2, but not in the heat-treated Plates P3 to P6.
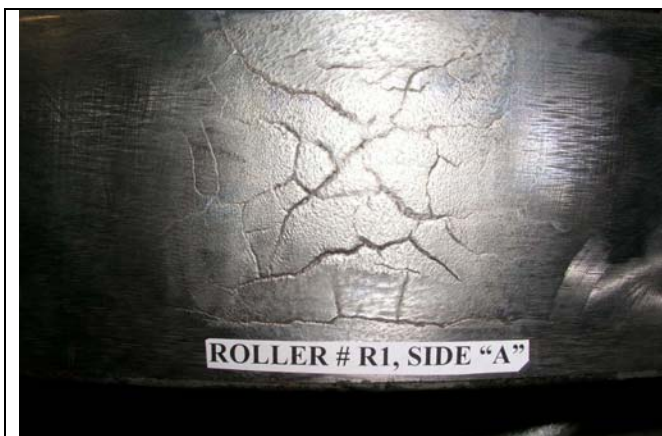

Fig. 9. Contact area of Wheel R1, Side A, after 1 million cycles

Fig. 10. Contact area of Wheel R2, Side A, after 220,000 cycles

Conclusions

The test results demonstrated clearly that the cast iron wheel performed very poorly under cyclic loading forming cracks in the contact area. The non-heated roller path plates also performed very poorly. The forged steel wheels and the heat-treated roller path plates, on the other hand, performed well.

Acknowledgement

References

1. Polyzois, D. and Muzyczka, W. J., (1994), Behavior of Cast-Iron Spillway Gate Wheels, *Journal of Materials in Civil Engineering,* Vol. 6, No. 4, pp. 495-512

2. Noonan, N. G., and Strange, W. H., (1934) Tests on Rollers, Technical Memorandum No. 399, U.S. Bureau of Reclamation, Denver, Colorado

3. Thomas H. R., and Hoersh, V. A., (1930), "Stresses Due to the Pressure of One Solid upon Another" Bulletin of Engineering Experiment Station, No. 212, University of Illinois, Urbana, Illinois

4. Boresi, A.P., Schmidt, R.J., and Sidebottom, O.M., (1993), Advanced Mechanics of Materials, 5th ed., John Wiley & Sons, Inc., New York